.

Parametric Validation Reinforcement Loops, and the Cosmological Constant Problem

Arthur E. Pletcher[1]
[1] *International Society for Philosophical Enquiry, Winona, Minnesota, USA*

email: artpletcher@ultrahighiq.org

Abstract

The primary consideration of this unifying field theory is the partial mapping of topology, within observations, as feedback loops. Specifically, the effective degrees of freedom (d.o.f.) resulting from such recursive exchanges. This modeling of observation as partial mapping seems well justified, as it is ubiquitous throughout nature's exchanges and propagation of information. Considered the meridian distortions of gnomonic projection of light waves in vision. Thus, PVRL extrapolates this same principle of constraining parameters in recursive feedback loops into the entire scope from QFT, (at flashpoint), to GR:

PVRL proposes a multispace of transitioning $\mathbb{R}n$ vector fields (similar to Hilbert space), coexisting like wavelengths in a prism. Progressing from quantum states, which are higher dimensional, outward to lower dimensional Macrospace (Note that backward causation is possible in quantum mechanics, but not possible in the constrained parameters of classic mechanics or GR). Familiar classic $\mathbb{R}4$ spacetime is just one phase of this multispace.

The mechanism which delineates between each state is PVRL: An iterated process of conscious binary gnomonic mapping of higher dimensional topology onto biased eigenstates. (and subsequent propagation within the quantum field). At each iteration, symmetry becomes more broken, and geometric parameters become more constrained (Polarity, bonding, separation, alignment and propagation). The inevitable outcome of such recursive feedback loops is a power law distribution (exponential tail), with increased entropy and complexity

The resolution of the Cosmological Constant Problem is an understanding that scales approaching QFT are viewed in higher dimensional divergence, and that scales approaching GR are viewed in lower dimensional convergence.

1. INTRODUCTION

The scope of a unifying theory is necessarily broad and defies any single starting point, as it requires conceptualizing an all inclusive idea.

It is axiomatic, that observations and interpretations are inherently biased, narrow and parametrically constrained, (which I model as partial mapping $f : M \rightarrow /(p_1, p_2)$ with consideration to reduced parameters in the image range, as compared with the codomain potential.). Equally ubiquitous, throughout nature, are the escalations and fluctuations (separations, bonding, aligments, ect) which result from such unresolvable discrepancies of $(a \cap b)^c$.

Therefore, it seems reasonable to base my supposition of validated conscious units (PVRL) on this universal principle, which suggests a self-validated pseudo-reality.

2. ZERO-POINT ENERGY, AS CALCULATED IN QFT

Partial Mapping Onto Lower Dimensional Vector Spaces

PVRL models observation as partial mapping with consideration to reduced parameters in the image range, as compared with the codomain potential.

Let open sets p_1 and p_2 be partial nonconformal gnomic mappings of sphere S onto two tangent planes at different (non-antipodal) surface parameters.

$$S \in \mathbb{R}^3_{def} = (x, y, z) \in \mathbb{R}^2 : ||x^2 + y^2 + z^2 = r|| \quad (1)$$

$$F : S \rightarrow /(p_1, p_2) \quad (2)$$

The projected geometry forms two disks with infinite horizons asymptotic to their respective meridians. From

a lower dimensional perspective of $\mathbb{R}^2$, the discs are separated. However, their horizons are connected from an $\mathbb{R}^3$ perspective. Note the delta (discrepancy) that exists between projected coordinate points within their respective open sets: Each non-antipodal disk shares a set of common points as well as a set of mutually separated points.

$$(p_1) \subset S \tag{3}$$
$$(p_2) \subset S \tag{4}$$
$$p_1 \cap p_2 \geq 1 \; and \; < p_1 \cup p_2 \tag{5}$$
$$p_1 \setminus p_2 \geq 1 \; and \; < p_1 \cup p_2 \tag{6}$$
$$(p_1 \cap p_2)^c > 0 \tag{7}$$

Distortions of meridians and orthodromes are given by:

$$x = \frac{\cos\phi \sin(\lambda - \lambda_0)}{cos\ c} \tag{8}$$
$$y = \frac{\cos\phi_1 \sin\phi - \sin\phi_1\ cos\phi\ cos(\lambda - \lambda_0)}{cos\ c} \tag{9}$$
$$where\ \cos c = \sin\phi_1\ sin\phi + \cos\phi_1\ cos\phi\ cos(\lambda - \lambda_0) \tag{10}$$

A similar gnomonic projection can be extend from a $\mathbb{R}^4$ hypershere onto two Spheres. As well, from a $\mathbb{R}^5$ hypersphere onto two $\mathbb{R}^4$ hyperspheres. These geometries are separated in their mutual $\mathbb{R}^n$ space. However, their geometry remains connected in their higher $\mathbb{R}^{n+1}$ space, with similar discrepancies and distortions.

Progression of Gnomonic Binary Mapping from QFT to GR

PVRL proposes a multispace of vector fields (Similar to a Hilbert Space), coexisting like wavelengths in a prism. Progressing from higher dimensional quantum states, outward to lower dimensional Macrospace (Note that backward causation is possible in quantum mechanics, but not possible in the constrained parameters of classic mechanics or GR). **Familiar classic $\mathbb{R}^4$ spacetime is just one phase of this multispace.** See figure 1.

Notice that Higher dimensions emanate from QFT onto progressively lower dimensions in GR. Familiar classic spacetime is at $\mathbb{R}^4$ and the parameters of macrospace, approaching the cosmic event horizon, become more constrained (Flattened) than classic space. (See figure 1). Thus, Scale magnitude is inversely proportionate to dimensionality:

$$||x||_2 \propto \mathbb{R}^{-n} \tag{11}$$

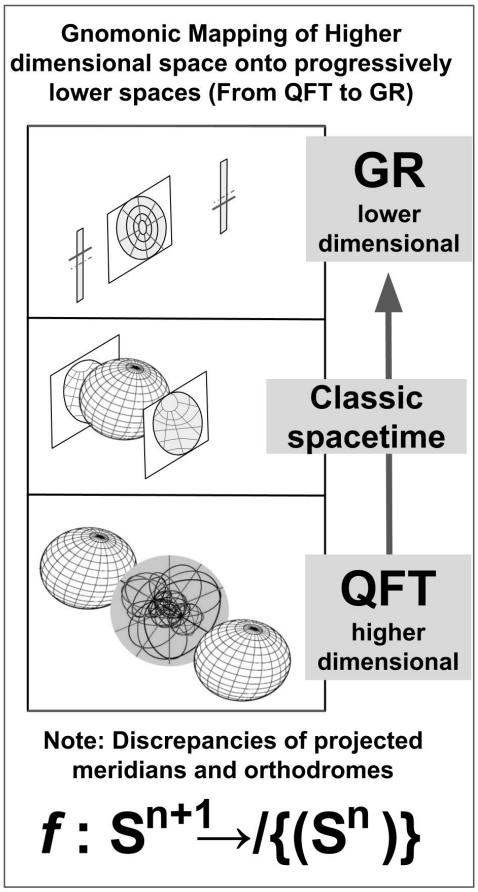

FIG. 1: Gnomonic mapping of higher dimensional space onto progressively lower spaces

In Section 4, I describe the mechanism (PVRL) which delineates and propagates the phases of these vector spaces. As well, the resulting broken symmetry, increasing entropy and reduced parameters.

The Diverging Effect in QFT

PVRL proposes a multispace with higher dimensions of scales approaching QFT. If so, a dimensional divergence would be expected, as observations approach Planck scales. Specifically, divergence in the time dimension $div\, t$ can be expressed as:

$$div\, t = \frac{\partial t_1}{\partial x_1} + \frac{\partial t_2}{\partial x_2} + \dots \frac{\partial t_n}{\partial x_n} \tag{12}$$

Particles in multiple time and positions would be observed simultaneously such that: **A range of position and time would appear as a dense mass in a single**

moment (Like an orbital), similar to observing a time lapsed photographed image.

Imagine an $\mathbb{R}^2$ disk observing an $\mathbb{R}^3$ sphere: An $\mathbb{R}^3$ curve is of x, y, z coordinates. However when this $\mathbb{R}^3$ geometry becomes gnomically projected / mapped onto the disk, it collapses to an $\mathbb{R}^2$ parametric reduced curve of x, y coordinates.

To view divergence in the time dimension is to view the past, present and future in a single instant (along with it's associated positions) appearing as a semi dense solid. So, a projectile will be viewed as an arc. By extension, an orbit will appear as a disk.

(Note that my theory correctly predicts that orbital scattering to be more dense toward the center, as the orbit paths are more frequent, which increases the probability density function.)

By further extension, consider observations from $\mathbb{R}^5$ geometry of x_1, x_2, x_3, x_4, x_5 collapsed (Gnomically mapped) onto $\mathbb{R}4$ geometry of x_1, x_2, x_3, x_4: An $\mathbb{R}^5$ projectile might appear as a partial torus, and so $\mathbb{R}^5$ Ψ_0 might appear as an s-orbit (With density increasing toward the center). See figure 2

Time divergence in QFT challenges the particle mass in DeBroglie's λ by substituting a unit of length, such as r_e (electron radius) or r_0 (atomic radius), instead of mass:

Hydrogen atom wave function in summation form:

$$\Psi_{\vec{k}(\vec{r})} = e^{i\vec{k}\cdot\vec{r}} \tag{13}$$

Using $p = \hbar k$ for momentum, the dominate wave function $Psi_{\vec{k_0}}$ includes wave vector $\vec{k_0}$:

$$k_0 = \frac{2\pi}{\lambda_0} \tag{14}$$

This use of scale, instead of mass, for λ resolves the following with greater parsimony:

- The use of mass, in massless photons
- Electron decay, by understanding electron shells as $\mathbb{R}^5$ topology mapped onto $\mathbb{R}^4$ spacetime
- Quantum "time travel" interaction with past and future, as divergence in the time dimension (viewed from $\mathbb{R}^4$ to $\mathbb{R}^5$.
- Backward causation.
- Gaps between orbitals.

See figure: 3

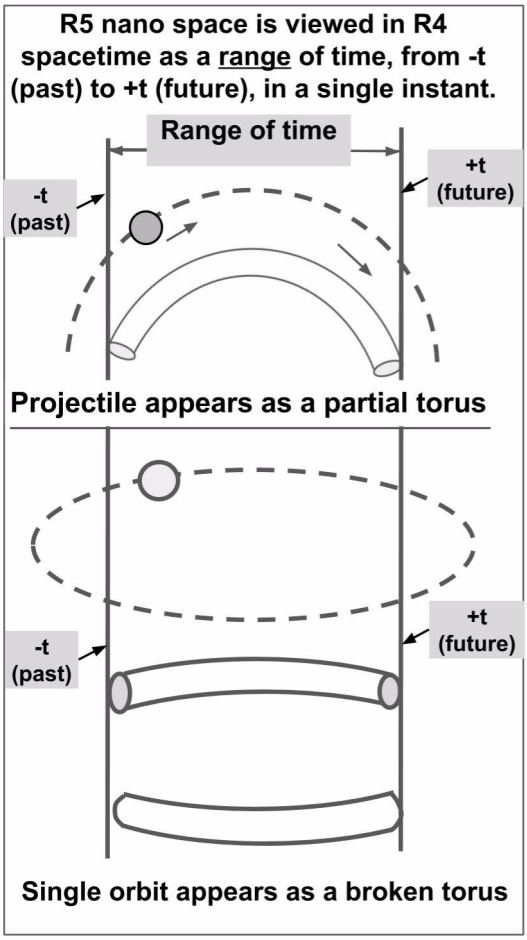

FIG. 2: $\mathbb{R}^5$ nano space is viewed in $\mathbb{R}^4$ spacetime, as a range of time from -t (past) to +t (future), in a single instant.

In section 4, I describe how mass is propagated into the quantum field through the iterative process of PVRL

Resolution to The Cosmological Constant Problem Λ in QFT

In equation 11, scale (from QFT to GR) is shown with a corresponding inverse dimensionality:

$$||x||_2 \propto \mathbb{R}^{-n}$$

Similarly, in equation 14, atomic or particle radius is used in λ instead of mass. Thus, λ is inversely proportionate to scale:

$$\lambda \propto r^{-e}$$

Thus, Λ behaves exactly as PVRL would predict; Measuring with increasing values, as volume decreases.

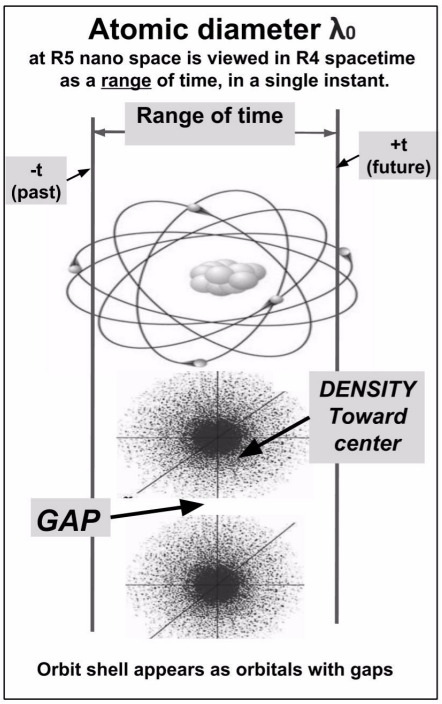

FIG. 3: Atomic diameter viewed in time divergence

To reiterate, PVRL views microscales with increasing divergence, as an effect of higher dimensionality. A range of time and position are viewed in a single instant

As well; A range of energy, time, momentum and position are not only observed, in brief moments at ground state, they are also measured with a **range of energy**. This energy represents multiple units of volume in one single flash.

Thus, **The total energy in a volume of empty space is significantly less than the sum of it's measured units of energy!** This is due to overlapping of units represented in each measurement (Each measurement is a sum of multiple time and positions, viewed in a single flash, in higher dimensional space) (See figure 4).

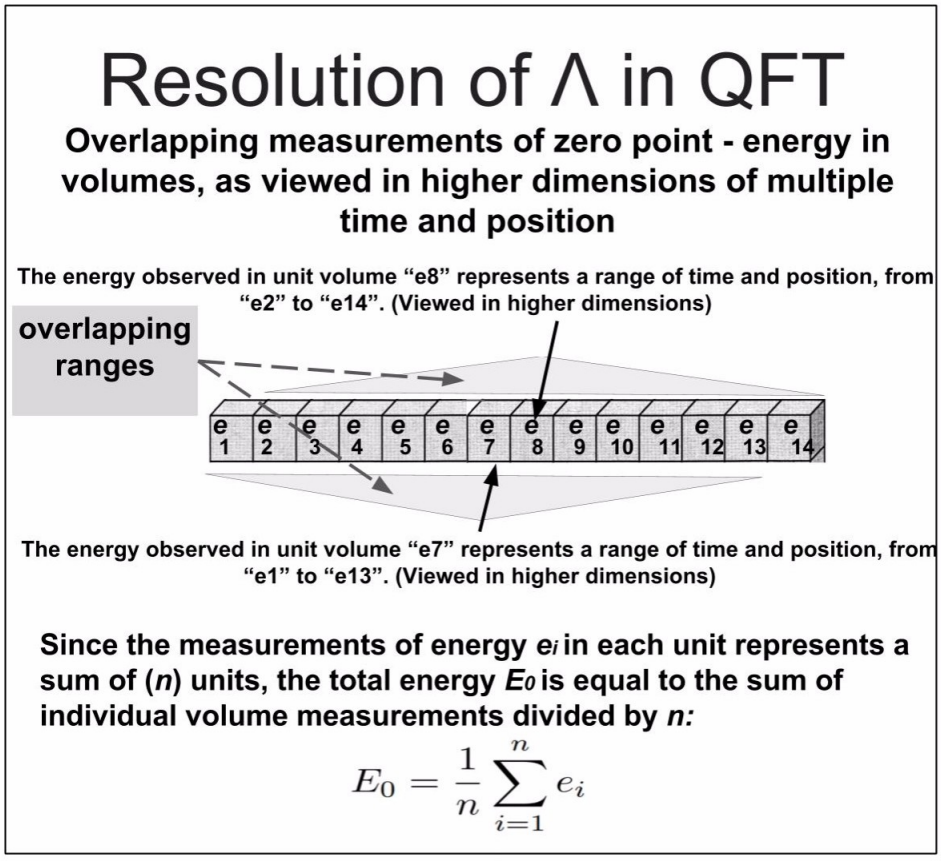

FIG. 4: Overlapping ranges of measured vacuum energy

Since the measurements of energy e in each unit represents a sum of n units, the total energy E_0 is equal to the sum of individual volume measurements divided by n:

$$E_0 = \frac{1}{n}\sum_{i=1}^{n} e_i \tag{15}$$

A test to demonstrate this "E_0 range theory" would be to construct multiple points of virtual photons, using two disks with spiral grooves, aligned in opposite amplitudes, (space at at min nanometers) to function as Casimir plates. Validation would be the result of energy e_n that is greater than the mean of it's local neighbors within x range on nanospace:

$$S^{'} = \{[e_{n-x}, \dots e_{n+x}]\}, \tag{16}$$

$$x = range\ of\ local\ vacuum\ states\ (undetermined) \tag{17}$$

$$e_n > \overline{S'} \tag{18}$$

See figure 5

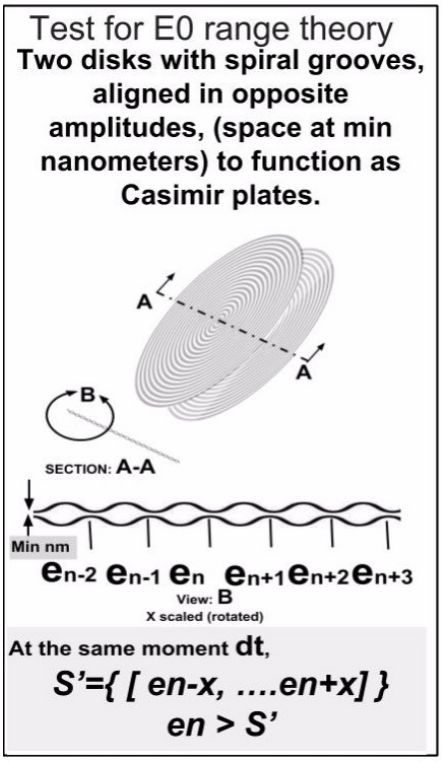

FIG. 5: Test for E_0 range theory

3. RESOLUTION TO THE COSMOLOGICAL CONSTANT PROBLEM Λ IN GR

The Flattening Effect of PVRL in GR

If my supposition of $\mathbb{R}^n$ multispace is correct, then observations of galaxies should indicate a dimensional convergence (due to the decreased dimensionality of macrospace compared with familiar classic space).

This convergence can be graphically represented in a $2D$ Euclidean coordinate system with converging number lines (Although they appear similar to log transformations, they represent an actual dimensional convergence). The rate of convergence corresponds to the cosmological constant Λ (2nd derivative of the Hubble constant: $\frac{\ddot{a}}{a} = H_\Lambda^2$) , in respect to universal expansion. In rotational curves, Λ is applied to r in local systems.

(Refer to figure 6): A theoretical galaxy rotation curve, as predicted by Kepler's laws is shown next to a typical observed galaxy rotation curve.

The apparent defiance of the inverse-square-law can be explained, alternatively to "Dark Matter", as a conventional orbital system viewed in converging dimension of time: As r increases, intervals of $\Delta\frac{v}{d}$ convergence within the local system.

The original regression line of the "Hubble Constant", from $0mpc$ to $45mpc$, is graphed (left) within my proposed converging dimension of time. A linear increase of velocity (acceleration) is apparent.

The same graph is shown (right) with a coordinate transfer to uniform time intervals, demonstrating a decreasing rate of acceleration approaching a constant

An equivalency is established between acceleration, as viewed in uniform dimension units, and velocity, viewed in converging dimension units. The graph on the right appears to be acceleration. However, a coordinate transfer would show a constant velocity.

4. PARAMETRIC VALIDATION REINFORCEMENT LOOPS

PVRL Interaction with the Quantum Field

The mechanism which delineates between each phase state is PVRL: An iterated process of conscious binary gnomonic mapping of higher dimensional topology onto biased eigenstates. (and subsequent propagation within the quantum field). At each iteration, symmetry becomes more broken, and geometric parameters become more constrained (Polarity, bonding, separation, proto-self reinforcement and alignment).

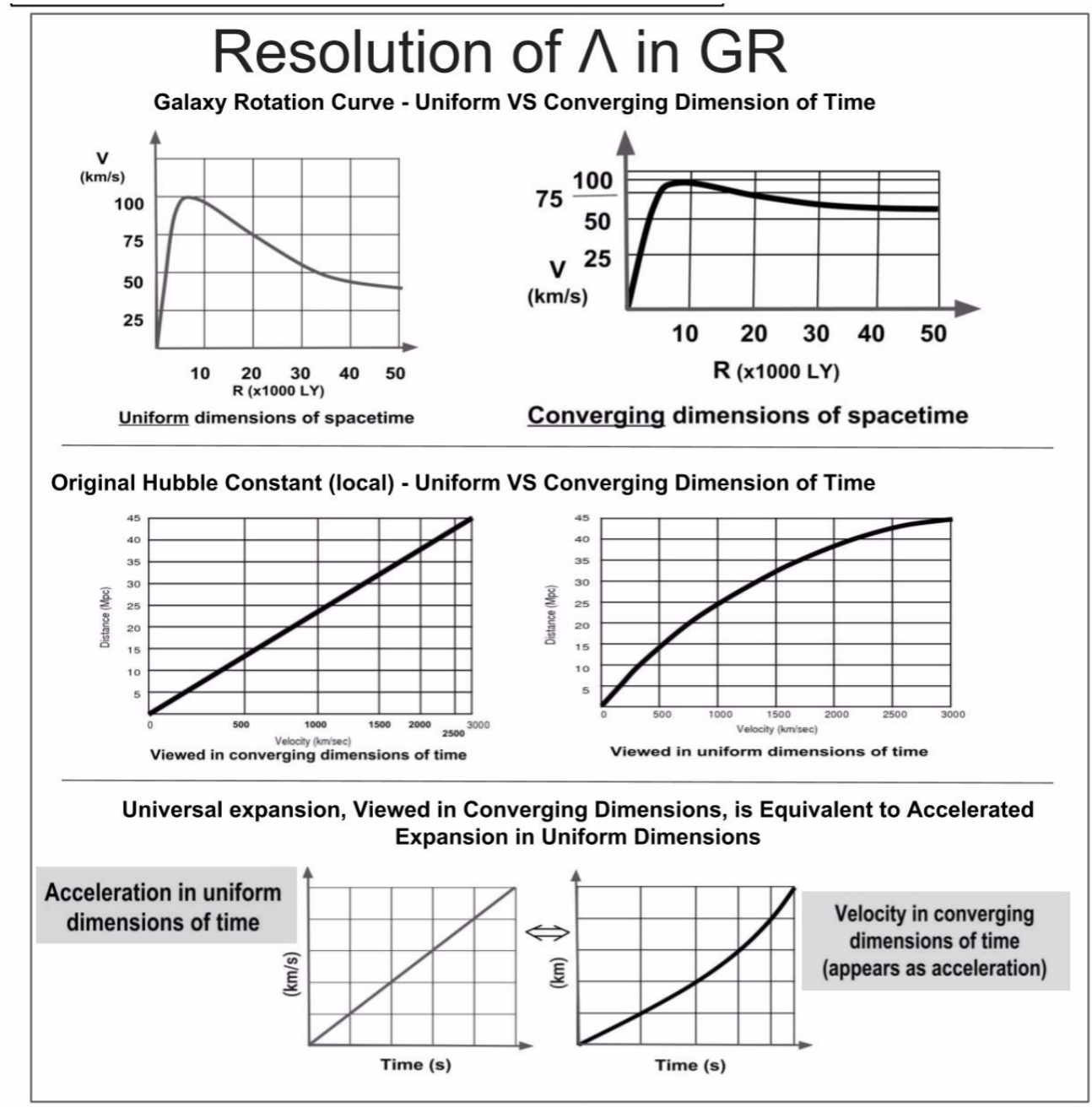

FIG. 6: converging dimensional space in GR

PVRL feedback loops are reinforcing, as opposed to control loops which maintain a set point. The interactions tend to escalate and deviate as a consequence of the discrepancies between their respective topologies. (Note that this same basic format is ubiquitous throughout nature.)

PVRL interacts with the quantum field, through propagation (From QFT to GR) to increasing scales, with subsequent emerging vector spaces (including familiar classic space). The basic components are shown in figure 7.

A and B can be regarded as rational agents in classic spacetime. However, on a more fundamental level, as operators in a vector field.

Their inherent discrepancy can not be resolved within the emerging $\mathbb{R}^n$ space. Thus A's perceptions / interpretation of B is always skewed and vice-versa. Consequently, reciprocating responses (Following the principle

of minimum energy, to maintain a state of homeostasis) increase exponentially (equation 22) in a vicious cycle. A functional space emerges from homogeneous topology which can be represented as divergence in a vector field. Note each partial derivative corresponds to n of $\mathbb{R}^n$ space:

$$div\,\vec{v} = \nabla \cdot \frac{\partial v_1}{\partial x_1} + \frac{\partial v_2}{\partial x_2} + \dots \frac{\partial v_n}{\partial x_n} \tag{19}$$

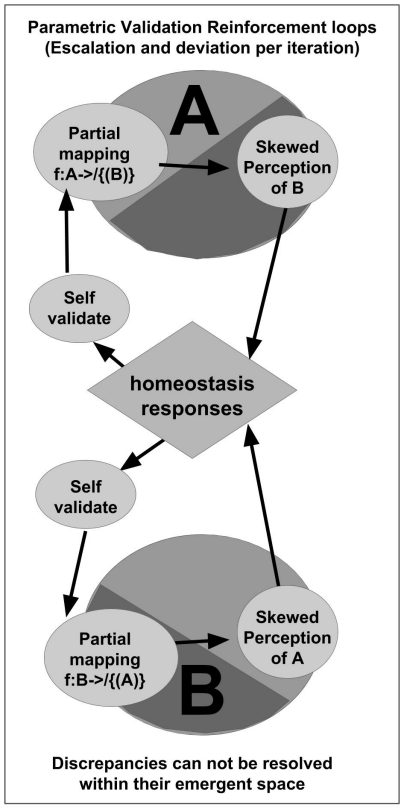

FIG. 7: Parametric Validation Reinforcement Loops

A density emerges between agent with similar topologies, represented as negative divergence.

The amount of energy required to ascend the resulting vector space is represented as the gradient.

$$\nabla f(x_1, x_2, \dots x_n) = \begin{bmatrix} \frac{\partial f}{\partial x_1} \\ \frac{\partial f}{\partial x_2} \\ \dots \\ \frac{\partial f}{\partial x_n} \end{bmatrix}$$

Decreasing Parameters of Recursive PVRL

Equation 22 describes the exponential development of PVRL. Dynamic field interactions (Divergence, convergence and bifurcation) are subsequently propagated, through alignments of charges. The inevitable result of such recursive exchanges is a decline of information (topology) with each iteration, forming a power law distribution with associated increased entropy. As scales increase, spacetime, symmetry and dimensionality are greatly diminished (See figure 8).

Power law of recursive exchanges

$$p(x) = Cx^{\alpha} = \frac{C}{x_{\alpha}},\ for\ x \geq x_{min}$$

$Normalization for\ (\alpha > 1)$

$$1 = \int_{x_{min}}^{\infty} p(x)dx = C\int_{x_{min}}^{\infty} \frac{dx}{x^{\alpha}} = \frac{C}{\alpha - 1} x_{min}^{-\alpha+1}$$

$$C = (\alpha - 1)x_{min}^{-\alpha+1}$$

Power law probability function (PDF)

$$p(x) = \frac{\alpha - 1}{x_{min}}\Big(\frac{x}{x_{min}}\Big)^{\alpha}$$

[1]

Per the Entropy-Power Inequality:

$$exp(2h(X+Y)) \geq exp(2h(X)) + exp(2h(Y)) \tag{20}$$

[2]

Where X and Y are independent real-valued random variables and h(X) is the differential entropy of the PDF

This exchange and distribution can be conceptualized as similar to a tennis match: As player A dominates player B. With increasing gap between them, the subordinate player looses control, position and accuracy, to a point of failure.

The resulting field dynamics are the "reality" of human existence. However, it is not an objective independent reality. Rather an emergent pseudo-reality.

Self Validated Pseudo-Realities

In order to understand PVRL and gnomonic projected emerging pseudo-realities, it is necessary to accept that, within each $\mathbb{R}n$ space, "objective observations" are profoundly biased and self-validated. The most familiar example of this phenomena is in the dynamics of dysfunctional partisan politics.

The following real-world example is a hypothetical tribal rivalry. Note that PVRL in Human interaction follows the same basic format as in figure 7, only more

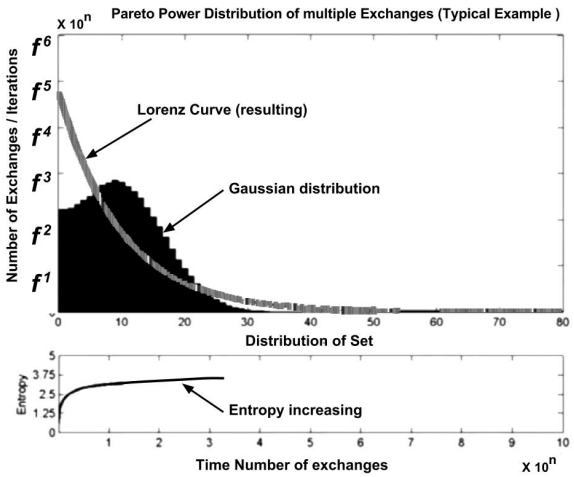

FIG. 8: Typical Pareto distribution from Gaussian, after multiple exchanges

sophisticated (Interpretations are biased projections, as in the Rorschach Test):

Two tribes, A and B, are engaged in some dispute. Both tribes seek a state of homeostasis. However, their innate mutual discrepancy (represented as the complement of $(A \cap B)^c$) , defies resolution (Refer to figure 9):

Let $g_i =$ *their initial mutual discrepancy* $(A \cap B)^c > 0$
Let $\alpha_i =$ *their mutual initial assessment*
Assume negative value $(a_i < 0)$

The following sequence emerges:
At iteration $f :^1$**,**

1. $F : B \to /A$
2. A views B's position with an initial bias of $-\overrightarrow{g_i}$
3. A responds with a shift of $+\overrightarrow{g_i}$
4. $F : A \to /B$
5. B views A's position as the sum of the initial $-\overrightarrow{g_i} + -\overrightarrow{g_1} = -\overrightarrow{2g_i}$
6. B reciprocates with a shift of $+\overrightarrow{2g_i}$

Mutually, α is validated (self-validated)

α increases to $\alpha_i(1 + \frac{1}{k})^2$

At iteration $f :^2$**,**

1. $F : B \to /A$
2. A views B's position with a resulting bias of $-\overrightarrow{3g_i}$
3. A responds with a shift of $+\overrightarrow{3g_i}$
4. $F : A \to /B$
5. B views A's position as the sum of $-\overrightarrow{2g_i} + -\overrightarrow{2g_1} = -\overrightarrow{4g_i}$
6. B reciprocates with a shift of $+\overrightarrow{4g_i}$

Mutually, α is validated (self-validated)

α increases to $\alpha_i(1 + \frac{1}{k})^3$

Through iteration $f :^n$**:**
$[\dots]$

The discrete form of this process is expressed as:

$$div_n = \sum_{i=1}^{n}(4i-1)(\alpha(1+\frac{1}{k})^n \tag{21}$$

However, PVRL regards these iterations to be occurring minutely at every moment, approaching a continuous function of:

$$div_n = (4n-1)\alpha_i e^{kn} \tag{22}$$

Generalized Dynamics of PVRL

This real-world narrative is just one emergent phase of PVRL. The same format of six step sequence cycles are common throughout the cosmos, from QFT to GR, with increasing sophistication and complexity.

Notice two separate narratives driving this system expansion. A's self validation of B's response is predicated upon B's self validation of A's response. Neither narratives are independently derived.

PVRL regards this self-validation to be $\equiv \forall$ **of perceived realty, and the resulting dynamics (of separation, bonding, alignment, diminishing propagation of information and proto-self) as the functional field parameters at every emergence space in** $\mathbb{R}^n$ **multispace**.

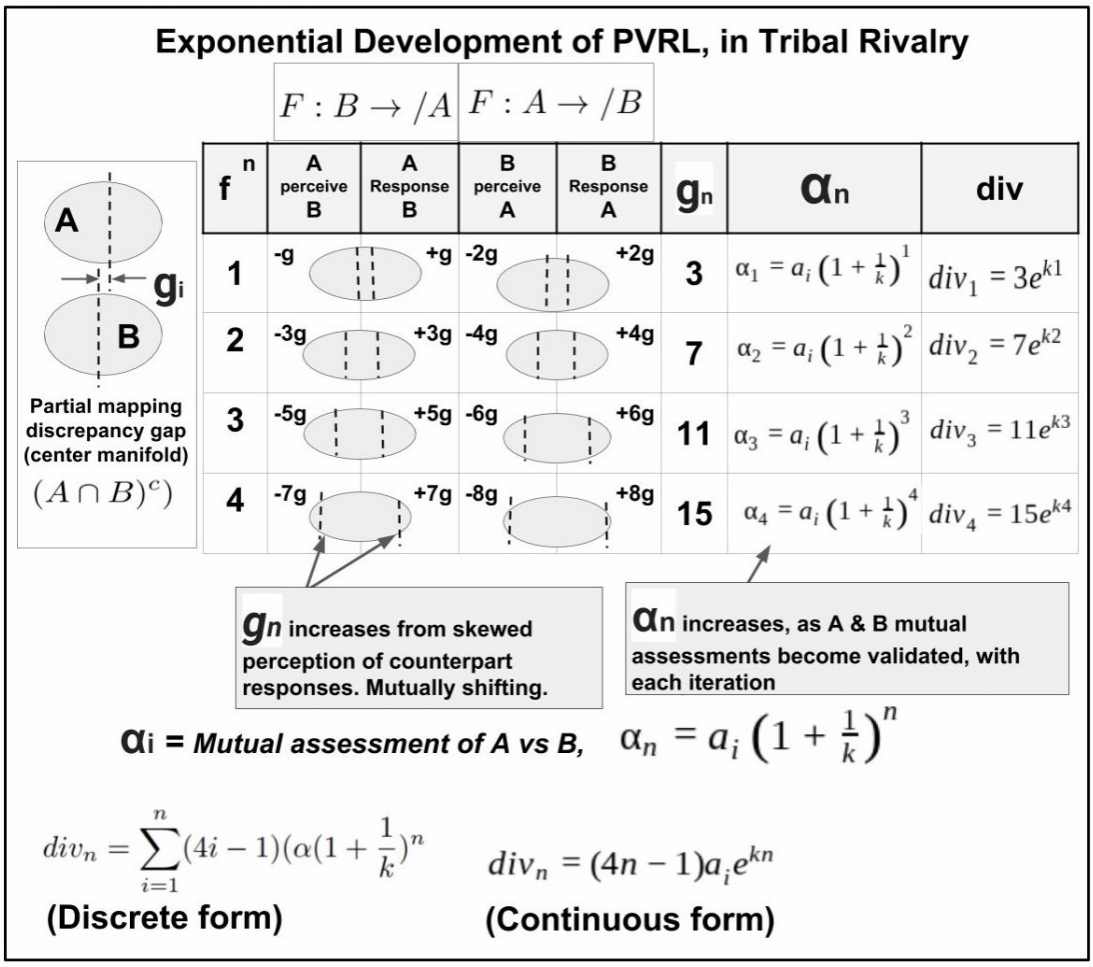

FIG. 9: Tribal dispute

Proto-Self Reinforcement at Collapse

PVRL recognizes that the "self" is contextual and developed in feedback loops. For example: I am a different self with my peers, than with my child, or with my parent. Also, the degree of self perception varies in context: I can become more self conscious when threatened by opposition, as well as less selfish in a bonding relationship.

Thus, the perception of a separated self (and free will) can be regarded as a function of PVRL, rather than the independent variable.

PVRL explains wave collapse as a dichotomy (from the initial flash-point) between the observer and particle.

Initially, the observer and particle are connected in a dimensionaly higher space. When an apparatus (detector) is introduced, intermediately, a link of observation and validation (PVRL) becomes closed, similar to a circuit. The initial dichotomy occurs in $\mathbb{R}^5$ space, then is propagated to $\mathbb{R}^4$ spacetime as an observer and particle duality of this propagation process. Validation is a necessary and critical component

5. CONCLUSION: CONNECTIONS IN $\mathbb{R}^n$ SPACE

PVRL proposes that the existence of nonlocality, causation and forces are local associations / connections in higher dimensions approaching QFT. Thus, all matter is connected in higher dimensions, resulting in the effects of gravitational fields in $\mathbb{R}^4$ spacetime. Nonlocality is a connection at an even higher space.

The simple idea is congruent with the basic supposition that: As $(a \cup b)^c$ increases, topology exchange decreases in the PVRL sequence. In higher dimensional / higher symmetry space (approaching QFT), locally connected nodes are maintained in iterations. However, as propagation progresses outward (toward GR) information integrity decreases, resulting in higher symmetry and reduced dimensionality. As a corollary, the field dynamics

(diversion, conversion, bifurcation and alignment) conform to local node connections in proportion to d distance. (the inverse square law).

In equations 1 thru 10, I described how the gnomonic projection of an $\mathbb{R}^3$ spherical manifold (S) onto an $\mathbb{R}^2$ plane (p_1) forms a disk with an infinite horizon, asymptotic to it's meridians (or othodromes):

$$S \in \mathbb{R}^3_{def} = (x, y, z) \in \mathbb{R}^2 : ||x^2 + y^2 + z^2 = r||$$
$$F : S \to /p_1$$

As PVRL views GR as a gnomic projection (of higher dimensions) onto a flattened disk, with typical meridian distortions, including the cosmic event horizon as the projected asymptote. A fascinating corollary is: that connections in Cosmology are reflected in most every classroom wall. The common world Atlas (With a Mercator projection at 82S and 82N.), which places the East Siberian Sea to be at opposite extremes from the Bering Sea, fails to account for their actual connection at the Bering Strait. PVRL proposes, by extension, that the outer extremes of GR are connected at the cosmic event horizon. **This geometry is congruent with General Relativity and Einstein's field equations. The only distinction is that the metric tensor indices: μ and ν must transition (at the extreme boundaries of the entire scope), from 5 dimensions, in QFT to 3 dimensions in GR. So, the amount of equations also must vary accordingly.**

[1] M. E. J. Newman. Power laws, pareto distributions and zipfs law. *Contemporary Physics*, 2005.

[2] Shannon Claude. *A Mathematical Theory of Communication*. Bell Syst, 1948.